LOAD-SETTLEMENT BEHAVIOR OF GEOMETRIC SHAPES ON SILTY CLAY

by

Osman I. Ghazzaly
William R. Cox

Prepared for

NATIONAL AERONAUTICS AND SPACE ADMINISTRATION

Langley Research Center
Hampton, Virginia

Contract NsG-604

THE UNIVERSITY OF TEXAS

DEPARTMENT OF CIVIL ENGINEERING

Austin, Texas

August, 1967

PREFACE

This study was sponsored under Grant NsG-604, An Investigation of Soil Modeling Problems Related to Impact Studies, from the National Aeronautics and Space Administration, Langley Research Center, Hampton, Virginia. Mr. M. E. Hathaway of Langley Research Center was technical monitor of the Grant.

Field tests were under the direction of Dr. Lymon C. Reese. Mr. Olen L. Hudson assisted with field testing and with laboratory testing of soil samples.

ABSTRACT

A series of static load-settlement tests was performed on two circular plates, two spheres, and a cone on the surface of a silty clay in the field. Based on the experimental findings, empirical relations were established expressing the load-settlement and bearing capacity-settlement behavior for the various foundation elements. These relations may be used to predict behavior for elements of different sizes under similar conditions.

For circular plates a comparison is made of theoretical and experimental values of ultimate bearing capacity, immediate settlements, and modulus of subgrade reaction.

A method is suggested for predicting the ultimate bearing capacity of a surface sphere in clay.

TABLE OF CONTENTS

Page

LIST OF TABLES

LIST OF FIGURES

SYMBOLS AND NOTATIONS

A	= area
A_s	= surface area of sphere
B	= width, or diameter, of footing
c	= cohesion
D	= depth to foundation level
E	= modulus of deformation
L	= length of footing
N_c, N_q, N_γ	= bearing capacity factors for general shear failure
N_c', N_q', N_γ'	= bearing capacity factors for local shear failure
P	= load
P_i	= load at the end of the initial straight line portion of the load-settlement curve
P_o	= ultimate load
P_s	= load at end of seating portion of the load-settlement curve
q	= pressure, stress, or bearing capacity
q_i	= bearing capacity at the end of the initial straight line portion of the bearing-capacity settlement curve
q_o	= ultimate bearing capacity
q_s	= bearing capacity based on surface area of sphere
S	= settlement
S_i	= settlement at the end of the initial straight line portion of the bearing-capacity settlement curve
S_o	= settlement at which ultimate bearing capacity occurs
S_s	= settlement at end of seating portion of the load-settlement curve
$S_{o.50}$	= settlement at 50% of ultimate bearing capacity

Y = settlement

γ = unit weight of soil

ϵ = strain

$\epsilon_{0.50}$ = strain at 50% of maximum stress

k = modulus of subgrade reaction, slope of pressure-settlement curve

k_1 = modulus of subgrade reaction for a 1.0 x 1.0 ft surface footing

k_B = modulus of subgrade reaction for a square surface footing of width B ft

k_i' = slope of the initial straight line portion of the load-settlement curve

k_f' = slope of final straight line portion of the load-settlement curve

μ = Poisson's ratio

σ = normal stress

σ_Δ = deviator stress

σ_3 = confinement pressure in triaxial test

τ = shear stress

ϕ = angle of internal friction

CHAPTER I

INTRODUCTION

1.1 General

A laboratory investigation of static load versus settlement was made by Iliya[1] for small plates, spheres, and cones resting on sand. Similar models were used by Poor[2] in vertical impact on a field deposit of silty to sandy clay.

It was of interest to extend the work of Iliya[1] and Poor[2] by conducting static load-settlement tests on plates, spheres, and cones at the same field site used by Poor.

1.2 Purpose and Scope

This investigation is part of a study on the behavior of manned spacecraft when impacting on soils. The investigation is concerned with model foundation elements of shapes similar to impacting surfaces of manned spacecraft.

Load-settlement behaviors of foundation elements on soils are complex and for this reason little confidence can be given to theoretical investigations of the problem unless supported by experimental data. Full-size field tests are preferred but time and cost studies point to the desirability of model studies if scaling laws can be developed.

It is desirable to relate dynamic to static characteristics of soils. The reasons for this include the relatively large amount of data available on static properties of soils and the ease with which static properties of soils can be obtained as compared with present known techniques for obtaining dynamic properties.

The purpose of this investigation was to measure the load-settlement behavior of plates, spheres, and cones under static loads on a field deposit of silty clay. Information obtained from the tests will be used in subsequent studies on soil modeling problems. No comparisons are given in this report with results of tests by Iliya[1] and Poor[2] but comparisons have been made with theoretical analyses.

CHAPTER II

THEORETICAL BACKGROUND

2.1 General

This chapter is a brief summary of the main and important theories of soil mechanics that have to do with the present study. It includes a presentation of the basic concepts of bearing capacity as well as load-settlement behavior of soils. It is intended only as a summary rather than a detailed discussion. A more complete treatment of the subject was given by Iliya[1].

2.2 Bearing Capacity of Soils

A number of theories have been developed for the ultimate bearing capacity of soils. The most widely accepted, however, is the one given by Terzaghi[3,4,5]. For the case of general shear failure of long footings, Terzaghi gives the ultimate bearing capacity by the following equation:

$$q_o = cN_c + \gamma\, D\, N_q + 0.5\, \gamma\, B\, N_\gamma \qquad (1)$$

where

q_o = ultimate bearing capacity

c = cohesive strength of the soil

N_c, N_q, N_γ = bearing capacity factors which depend only on the angle of internal friction of the soil

γ = unit weight of the soil

D = depth from soil surface to bottom of footing

B = width of footing.

Values of N_c, N_q, and N_γ are given by Terzaghi[3,4,5].

General shear failure is the case when the load-settlement curve for a footing indicates a definite ultimate load. On the other hand, a local shear failure is characterized by a load-settlement curve that does not exhibit a peak load but continues to rise on a fairly straight line tangent. The ultimate bearing capacity in this latter case is arbitrarily chosen at the point where the curve passes into that straight tangent.

By analyzing the results of experimental studies, Terzaghi[4] developed empirical equations expressing the ultimate bearing capacity of circular and square footings. For general shear failures per unit area of footings these equations are:

Circular footings:

$$q_o = 1.3c\ N_c + \gamma\ D\ N_q + 0.3\gamma\ B\ N_\gamma \tag{2}$$

where B is the diameter of the footing.

Square footings:

$$q_o = 1.3\ c\ N_c + \gamma\ D\ N_q + 0.4\gamma\ B\ N_\gamma \tag{3}$$

where B represents the width of the footing.

The equations for local shear failure conditions are similar to formulas 2 and 3, except that 2/3 c is used instead of c, and N_c', N_q', and N_γ' are substituted for N_c, N_q, and N_γ in the two equations. Values for N_c', N_q', and N_γ' are given by Terzaghi[3,4,5].

Skempton[6] gives curves and tables for determining the bearing capacity factor N_c for strip, circular, and square footings in clay at various values of the ratio D/B. He also presents the following equation for computing N_c for rectangular footings:

$$N_c \text{ (rectangle)} = \left[0.84 + 0.16\,\frac{B}{L}\right] N_c \text{ (square)} \qquad (4)$$

where L is the length of the footing.

Peck[7] gives still another equation for computing the bearing capacity of foundations in clay.

Terzaghi's general equations can be used for the various conditions encountered in the field. For example, the ultimate bearing capacity for surface footings is obtained by substituting $D = 0$ in the equations. In the case of purely cohesive soils ϕ is set equal to zero, while for cohesionless soils c becomes equal to zero.

2.3 Load-Settlement Analysis of Footings

The elastic settlement of a loaded area on the surface of a soil can be determined using the theory of elasticity. Skempton[6] applied such methods, together with other simplifying assumptions, to derive the following equation expressing the immediate settlement of rigid circular footings in saturated clays:

$$Y = 2\,\epsilon\,B \qquad (5)$$

where

Y = immediate settlement

B = width of footing

ϵ = strain

The strain ϵ is determined from a stress-strain curve obtained in the laboratory by performing an unconfined compression test, or an undrained triaxial test. The value ϵ is chosen at any value of stress σ. The corresponding value of the settlement Y will be at a footing pressure q where $q/q_0 = \sigma/\sigma_{max}$. The bearing capacity of this footing is q_0 and the maximum stress of the laboratory stress-strain curve is σ_{max}.

The immediate settlement computed by Eq 5 is believed to be only accurate in the range within which the stress-strain curve is a straight line.

Terzaghi[8] presents a method for solving settlement problems using the theory of subgrade reaction. Values of the modulus of subgrade reaction k can be derived from actual field tests, or estimated from data published by Terzaghi[8] and others. The coefficient k is defined as the slope of the straight line portion of the pressure-settlement curve, and is assumed to be a constant for all points of the surface of contact.

CHAPTER III

TESTING EQUIPMENT AND PROCEDURE

3.1 Foundation Media

The entire series of static load-settlement tests was carried out in the field on a site at the Austin Country Club prepared by Poor[2]. The foundation material was a silty clay, classified as (CL) according to the unified classification system, with some organic material at the top few inches. Classification tests indicated that the soil within the test area was fairly uniform in moisture and composition. The selection and preparation of the test site is discussed fully in reference[2]. Soil classification and description are also presented in the same reference.

Because of heavy rains that continued for a number of days after completion of the dynamic drops, and prior to the start of the present series of static tests, moisture contents within the test area were generally about one to two percent higher than those reported by Poor[2] at the various depths. From the various moisture samples secured throughout the site it was concluded that the average moisture content for the top foot depth of the soil was about 16 percent. The maximum range of variation in moisture contents at this level was in the order of 1 percent.

The test program was accomplished in the shortest possible period to prevent any major change in soil moisture and conditions throughout this time. Because of the slight variation in the moisture content of the soil from that reported by Poor[2], undisturbed samples had to be secured at the end of the test program. These samples were used to determine the strength parameters of the top layer of soil at its new moisture condition. The sampling technique has been described by Poor[2].

The cores were obtained from positions close enough to the points where the static tests were performed, to represent actual conditions. Their location had also to be undisturbed during both the dynamic drops and static tests. The undisturbed cores were sealed tightly and transferred to the laboratory where they were carefully extruded, wrapped, and kept in the moist room until tested.

The diamter of the extruded undisturbed specimens was 2.8 in. Unconfined compression tests, and triaxial quick (undrained) compression tests at 3 and 5 psi confining pressures were performed on these samples in the laboratory. The test specimens, 2.8 in. diameter, were cut to 5.6 in. length. Sample preparation and test procedure were according to those generally used at the soil mechanics laboratory at The University of Texas[9].

The average results of the laboratory tests for all the specimens tested, representing the test area, are given in Figs. 1 and 2. Figure 1 shows the average stress-strain curves for the various confining pressures, σ_3, while Fig. 2 indicates the Mohr diagram and average shear strength for the top layer of the soil. The average cohesion c was 2.8 psi and angle of internal friction $\phi = 39^\circ$. The equation of the Mohr's envelope is:

$$\tau = 2.8 + \sigma \tan 39^\circ. \tag{6}$$

The modulus of deformation E is defined as the ratio of the stress to strain at any point on the laboratory stress-strain curve of the soil. The variation of E with strain and with confining pressures is indicated in Fig. 3, which is derived from the data in Fig. 1. It is observed that the modulus of deformation is contant for a certain region at the heart of the test and then decreases constantly until the end.

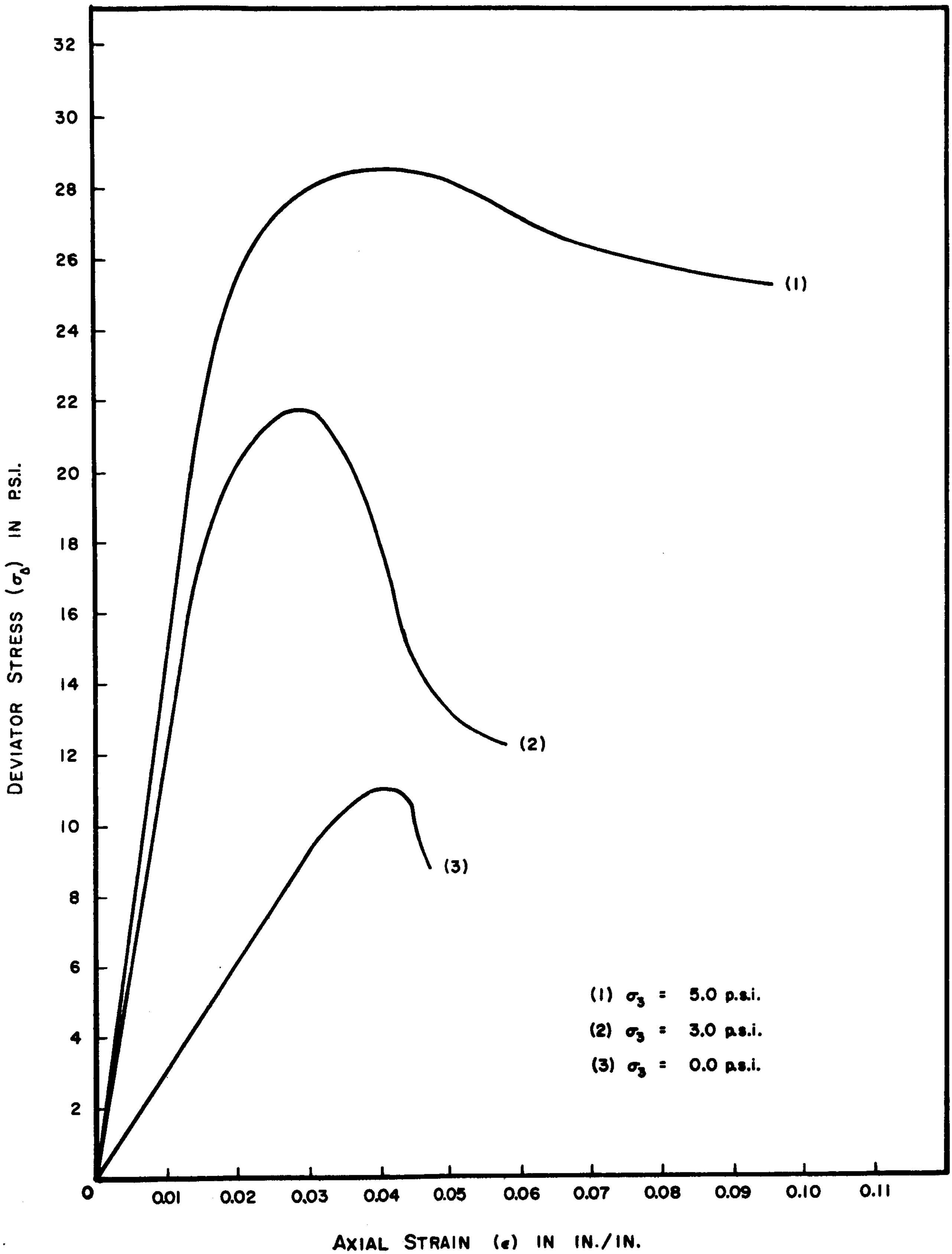

FIG. 1. STRESS-STRAIN CURVES FOR AUSTIN COUNTRY CLUB SILTY CLAY

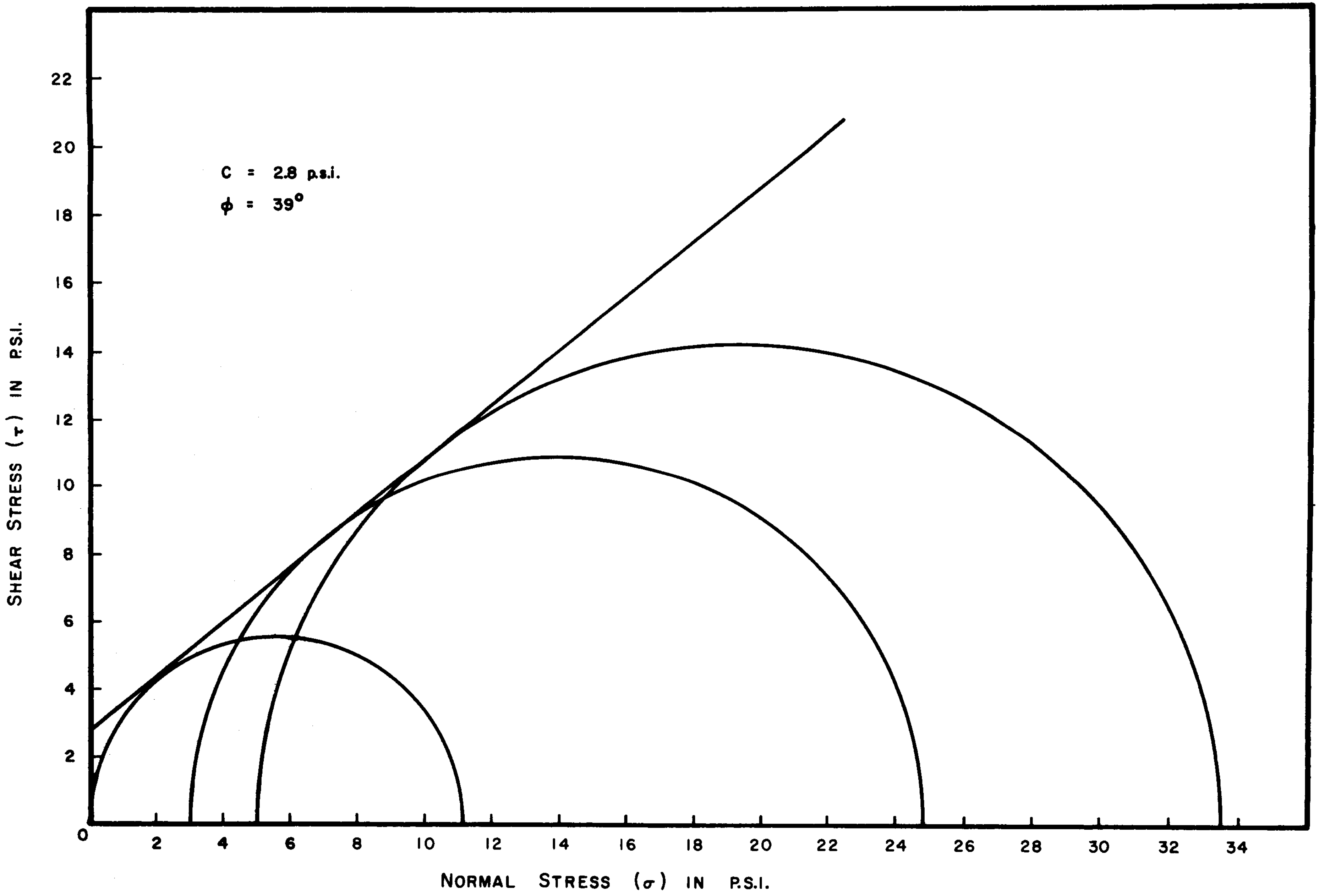

FIG. 2. MOHR'S CIRCLES AND ENVELOPE FOR AUSTIN COUNTRY CLUB SILTY CLAY

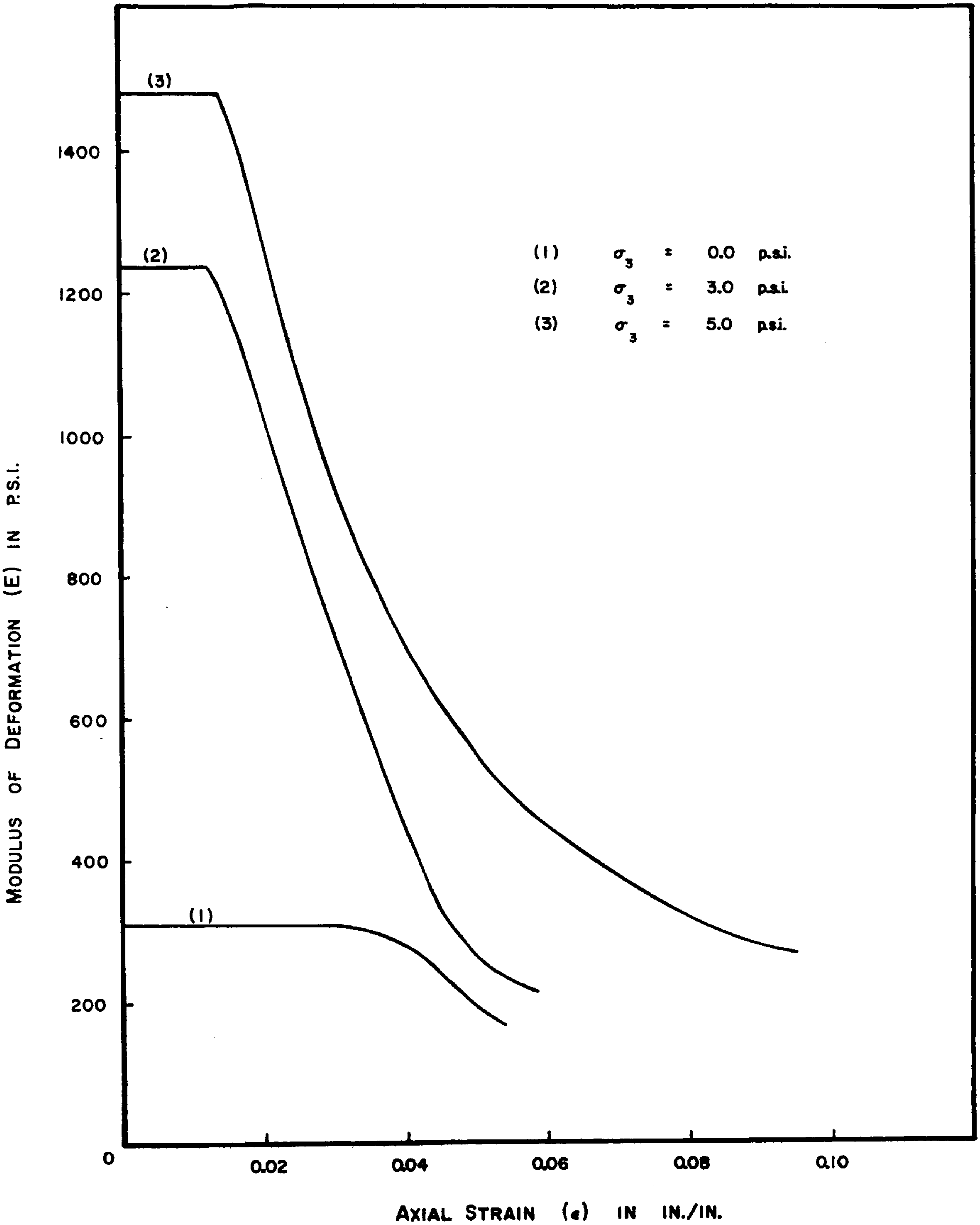

FIG. 3. MODULUS OF DEFORMATION vs. AXIAL STRAIN AT VARIOUS CONFINING PRESSURES FOR AUSTIN COUNTRY CLUB SILTY CLAY

Unit weight determination for a number of extruded samples was also performed following standard procedures. The average unit weight γ from these determinations was found to be about 120 pcf. The maximum range of variation in unit weights for all samples tested was in the order of 2.0 pcf.

Lateral strain-ratio determination for this soil can be accomplished, in the case of unconfined compression tests, using the procedure outlined by Ghazzaly[10] for clay specimens. Such tests were not performed in this investigation.

3.2 Model Foundation Elements

The foundation elements used in this investigation were the same ones selected by Iliya[1]. These included two circular plates 3.14 in. and 2.22 in. in diameter, two spheres of sizes 3.14 in. and 5.0 in. in spherical diameter, and a 60 degree right circular cone which was 3.0 in. high. Complete dimensions are given in Iliya's[1] Fig. 1.

The two plates were machined from aluminum blocks 0.5 in. thick. Their surface areas were in the ratio of 1 to 2. The spheres and cone were solid aluminum castings. All foundation elements used were considered to be rigid, since their deflections within the range of loads experienced in this investigation were negligible.

The selected model foundation elements provided the means for a study of size effects on the load-settlement behavior for each geometric configuration, and also enabled the comparison of such behavior for the various shapes of elements used.

3.3 Test Equipment and Setup

A flatbed 1.5 ton truck was used to support a driving screw jack and an electric motor that operated it. Figures 4 and 5 show the testing equipment. A concrete block weighing about one ton was placed on the bed of the truck to provide a reaction to loads picked up by the foundation elements during the series of field tests.

The driving screw jack was connected to a piece of a heavy steel channel, which in turn was bearing on the two beams at the bottom of the flat bed of the truck at its very end. The channel was tied securely to the truck to prevent any movement during loading. The dimensions of the heavy channel were such that its maximum deflection within the range of applied loads was negligible. The concrete weight was of sufficient size to prevent any movement of the bed of the truck during testing.

The screw jack had a 5.0 in. rise and 15.0 tons capacity (Model No. 111-c-2, Duff Norton Mfg. Co., Pittsburg, Pennsylvania). It was operated using an electric motor at a constant rate of 0.07 in. per min. At the end of the driving screw there was a circular plate to which a proving ring was fixed, as shown in Fig. 5. The proving ring had a capacity of 2000 lb and a sensitivity of 2.0 lb. The foundation elements tested were screwed to the bottom of the proving ring. The settlement was measured by a dial extensometer, as shown in Fig. 5, with 2.0 in. travel and 0.001 in. sensitivity. The extensometer was connected by means of a stiff steel rod to a firm stand in a position which was not affected by loading. All connections and elements were tight and rigid enough to prevent any deflection or movement.

The test setup was accurately checked to be sure that the driving screw was absolutely vertical during its entire thread, perpendicular to the upper face of the foundation elements, and exactly centered in the area of the element.

FIG. 4. FLATBED TRUCK WITH CONCRETE BLOCK ON TOP, TWO CHANNELS FIXED TO ITS BOTTOM, AND MOTOR AND JACK FIXED TO CHANNELS

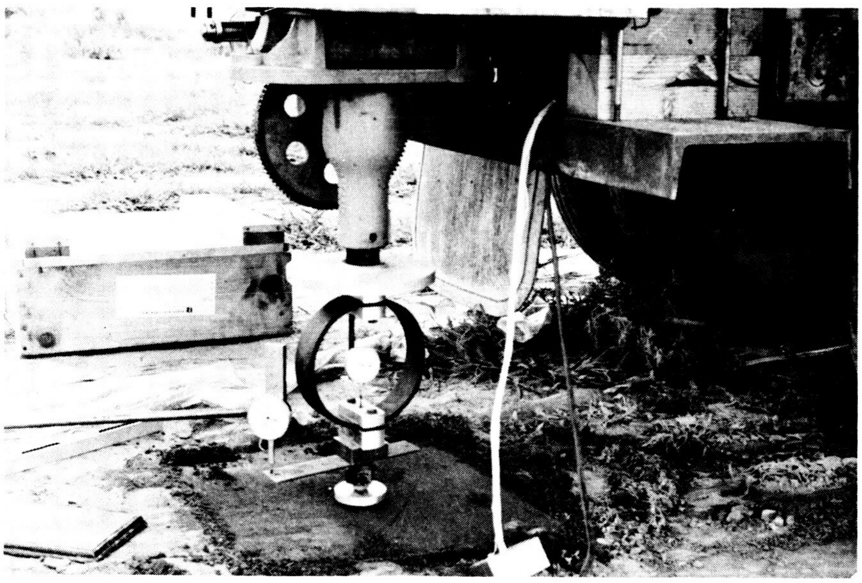

FIG. 5. TEST SETUP SHOWING CHANNELS, MOTOR, JACK, PROVING RING, EXTENSOMETER, PLATE, AND TRUCK

3.4 Test Procedure

The test setup described in the preceding article was used to run a series of load-settlement tests in the field. The particular foundation element to be tested was attached to the proving ring. The soil at the position of the test was cleared of all roots and organic matter at the top. The surface of the soil was then carefully leveled using a straight edge and care was taken to minimize soil disturbance at the top. The surface of the soil was checked to make sure that it was horizontal and that complete contact would occur with the foundation element.

After soil preparation, the truck was backed into position. The motor was operated and the foundation element lowered until it just touched the soil. The extensometer was then placed in position and both load and settlement dials set to zero. All these steps were accomplished in the shortest possible period of time to minimize evaporation of soil moisture.

At this point, loading was started and continuous readings of the proving ring and settlement extensometer taken. The speed of the motor, controlling the rate of loading, was such that a constant rate of settlement of 0.07 in. per min. was produced and maintained during all tests. This rate was recommended and used by Iliya[1], and is typical of all loading tests. The test was continued long enough and until the foundation element could no longer be treated as a surface footing. The loading was then stopped, motor reversed, and the foundation element raised. A moisture sample was immediately secured from the loaded area and sealed in a box that was taken to the laboratory for analysis.

CHAPTER IV

RESULTS AND DISCUSSION

4.1 Load-Settlement Tests on Plates

In this article the results of all tests performed on the circular rigid plates loaded at the surface of the soil are presented in detail. A discussion of the significance of these results is also given.

4.1.1 Load-Settlement Curves

The load-settlement curves for the two circular plates, 3.14 and 2.22 in. diameter, are shown in Fig. 6. The shape of these curves are similar with a straight line portion at the start, a curved portion at the middle, and a transition to a straight line tangent rising upwards. The shape of these curves indicates that it is a case of local shear failure where no definite ultimate load is apparent. As was discussed in Chapter II, the ultimate load for local shear failure is selected as the load corresponding to the point on the load-settlement curve where the curve passes into the straight line tangent. The ultimate load P_o is directly proportionate to the contact area of the plates.

Each experimental curve shown in this chapter is the average of the results of two identical tests. The tabulated results were read off these average curves.

Table 1 gives a summary of the load-settlement curves for the circular plates. It can be observed that the settlement S_o at which the ultimate load P_o occurred is directly proportional to the area of contact; also that the slope of the initial straight line portion of the load-settlement curve is directly proportional to the diameter of the circular plate.

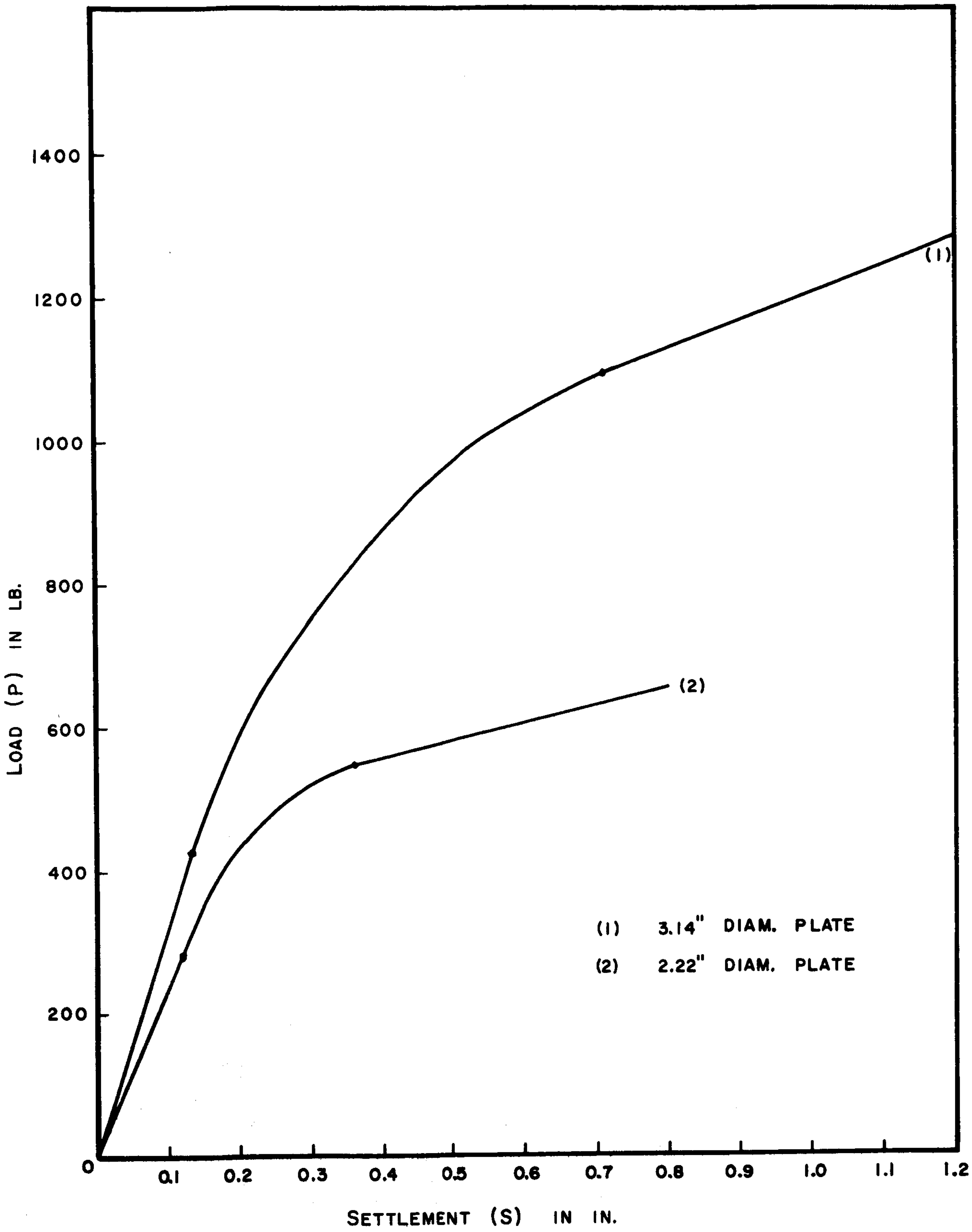

FIG. 6. LOAD - SETTLEMENT CURVES FOR CIRCULAR PLATES

TABLE 1

SUMMARY OF RESULTS OF LOAD-SETTLEMENT TESTS ON CIRCULAR PLATES

(A)

B Diameter of Plate in.	Ratio of Diameters Referred to Smaller Plate	Ratio of Areas Referred to Smaller Plate	P_o Ultimate Load lb	Ratio of P_o Referred to Smaller Plate	S_o Settlement at which P_o Occurred in.	Ratio of S_o Referred to Smaller Plate
2.22	1.000	1.000	547	1.000	0.360	1.000
3.14	1.414	2.0	1099	2.009	0.716	1.989

(B)

A Area of Plate in.^{2}	S_1 Settlement at End of Initial Straight Line in.	Ratio of S_1 Referred to Smaller Plate	P_1 Load Corresponding to S_1 lb	Ratio of P_1 Referred to Smaller Plate	k_1' Slope of the Initial Straight Line lb/in.	Ratio of k_1' Referred to Smaller Plate
3.87	0.121	1.000	274	1.000	2265	1.000
7.74	0.132	1.091	426	1.555	3227	1.425

4.1.2 Bearing Capacity - Settlement Curves

The bearing capacity q at any settlement S is computed by dividing the load P by the area of the plate A

$$q = \frac{P}{A} \quad . \tag{7}$$

Since A is a constant for any plate, the shape of the q-S curve is similar to that of the P-S curve, with the S-axis being the same in both. The bearing capacity-settlement curves are shown in Fig. 7, and values from these curves are given in Table 2.

There was a very slight increase in the value of q_o as the diameter of the plate increased. This increase is due to the fact that the silty clay has an angle of internal friction ϕ. For clays with $\phi = 0$ no increase in the value of q_o would be expected as the diameter of the plate increases.

The ratio S_o/B increased in direct proportion with the diameter of the plate. No definite pattern of variation could be detected for the ratio of the settlement S_i, at the end of the initial straight line portion of the curve, to the diameter of the plate B. The ratio S_i/B did not seem to be much affected by the diameter of the plate.

The value of the bearing capacity at the end of the initial straight line portion of the curve q_i was somewhat higher for the smaller plate. Again no definite pattern could be observed for the variation of the ratio q_i/q_o.

4.1.3 Modulus of Subgrade Reaction

The modulus of subgrade reaction k, defined as the slope of the initial straight line portion of the bearing capacity-settlement curve, was inversely proportional to the diameter of the plate, as shown in Table 2. If

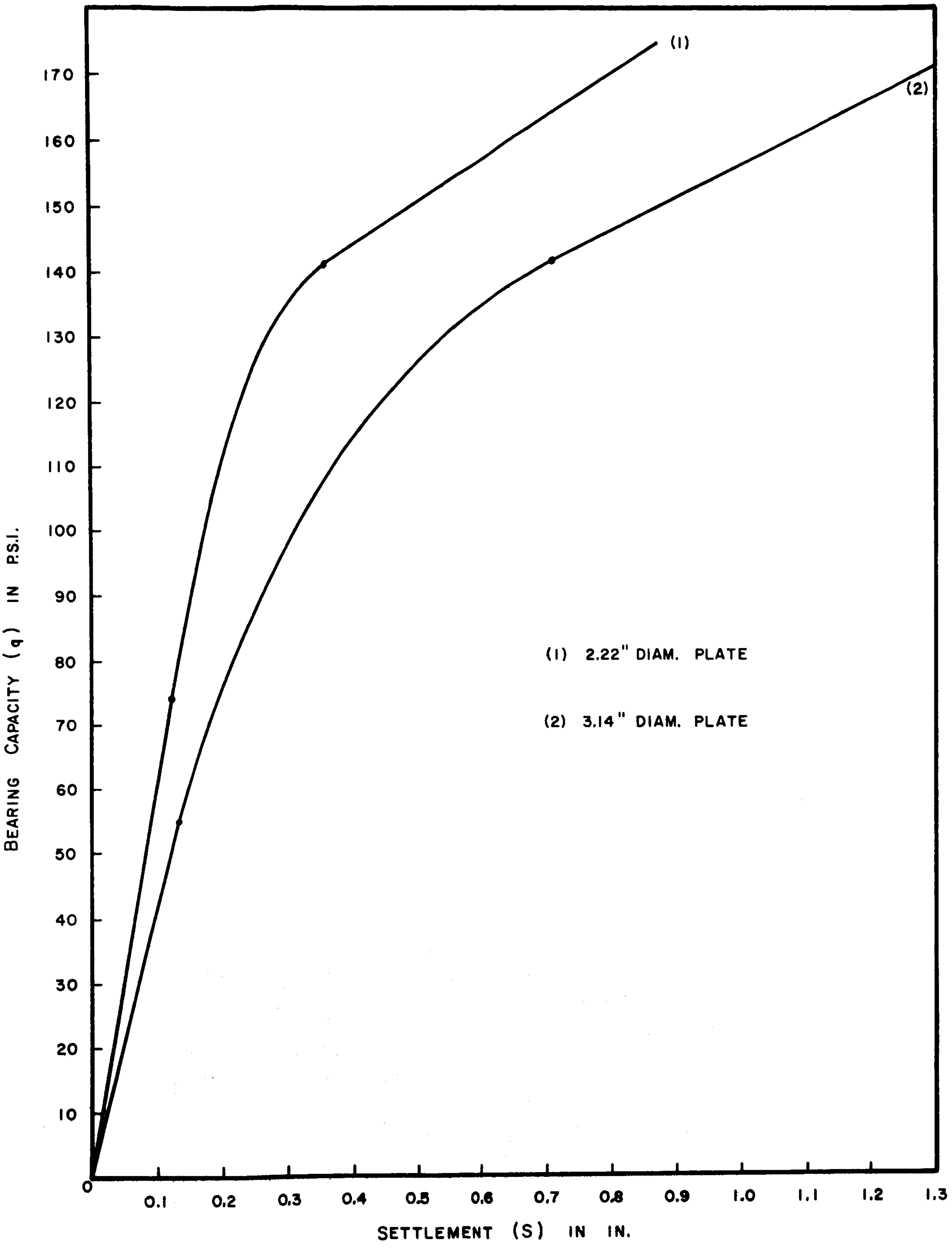

FIG. 7. BEARING CAPACITY VS. SETTLEMENT CURVES FOR CIRCULAR PLATES

TABLE 2

BEARING CAPACITY-SETTLEMENT RELATIONS FOR CIRCULAR PLATES

B Diameter of Plate in.	q_o*** Ultimate Bearing Capacity psi	S_o/B*	S_1/B*	q_1** Bearing Capacity at End of Straight Line psi	q_1/q_o	$k = q_1/S_1$ Modulus of Subgrade Reaction lb/cu in.	Ratio of k Referred to the Larger Plate	Ratio of q_o Referred to the Smaller Plate	Ratio of q_o Referred to the Larger Plate
2.22	141	0.162	0.055	70.8	0.501	585	1.403	1.000	1.287
3.14	142	0.228	0.042	55.0	0.388	417	1.000	1.007	1.000

* Values of S_o and S_1 are given in Table 1

** $q_1 = P_1/A$ (P_1 is given in Table 1)

*** $q_o = P_o/A$ (P_o is given in Table 1) the modulus of subgrade reaction is more generally defined as the ratio of the bearing capacity to the settlement at any point on the bearing capacity-settlement curve, it can be realized that this modulus k will not be constant throughout the entire range of the curve. The variation of k with settlement is shown in Fig. 8, which indicates that the modulus is only constant within a small range of settlements at the start of the test and then decreases constantly with the increase in settlement. The rate of increase, however, was much higher at the higher levels of settlement. At this point the similarity in shape between the curves for modulus of subgrade reaction in Fig. 3 should be noted.

4.1.4 Comparison of Experimental and Theoretical Results

Based on Terzaghi's theory, an expression for the ultimate bearing capacity of a circular footing at the surface of a silty clay (D = 0) and for local shear failure conditions can be determined from Eq 2.

$$q_o = 1.3 \left(\frac{2}{3} c \right) N_c' + 0.3 \, \gamma \, B \, N_\gamma' \quad . \tag{8}$$

Using values for N_c' and N_γ' as given by Terzaghi[4] for $\phi = 39^\circ$, and values of c and γ from Art. 3.1, the bearing capacities q_o for the two plates could be derived and are shown in Table 3.

Comparing the theoretical and experimental values of the maximum bearing capacity, it was concluded that the theoretical q_o is quite conservative. The average ratio of q_o (experimental) to q_o (theoretical) for the two circular plates investigated was found to be 1.746.

Skempton's[6] Eq 5 was used to calculate the settlement at 50 percent of the ultimate bearing capacity. The equation in this case becomes:

$$S_{0.50} = 2 \, \epsilon_{0.50} \, B \tag{9}$$

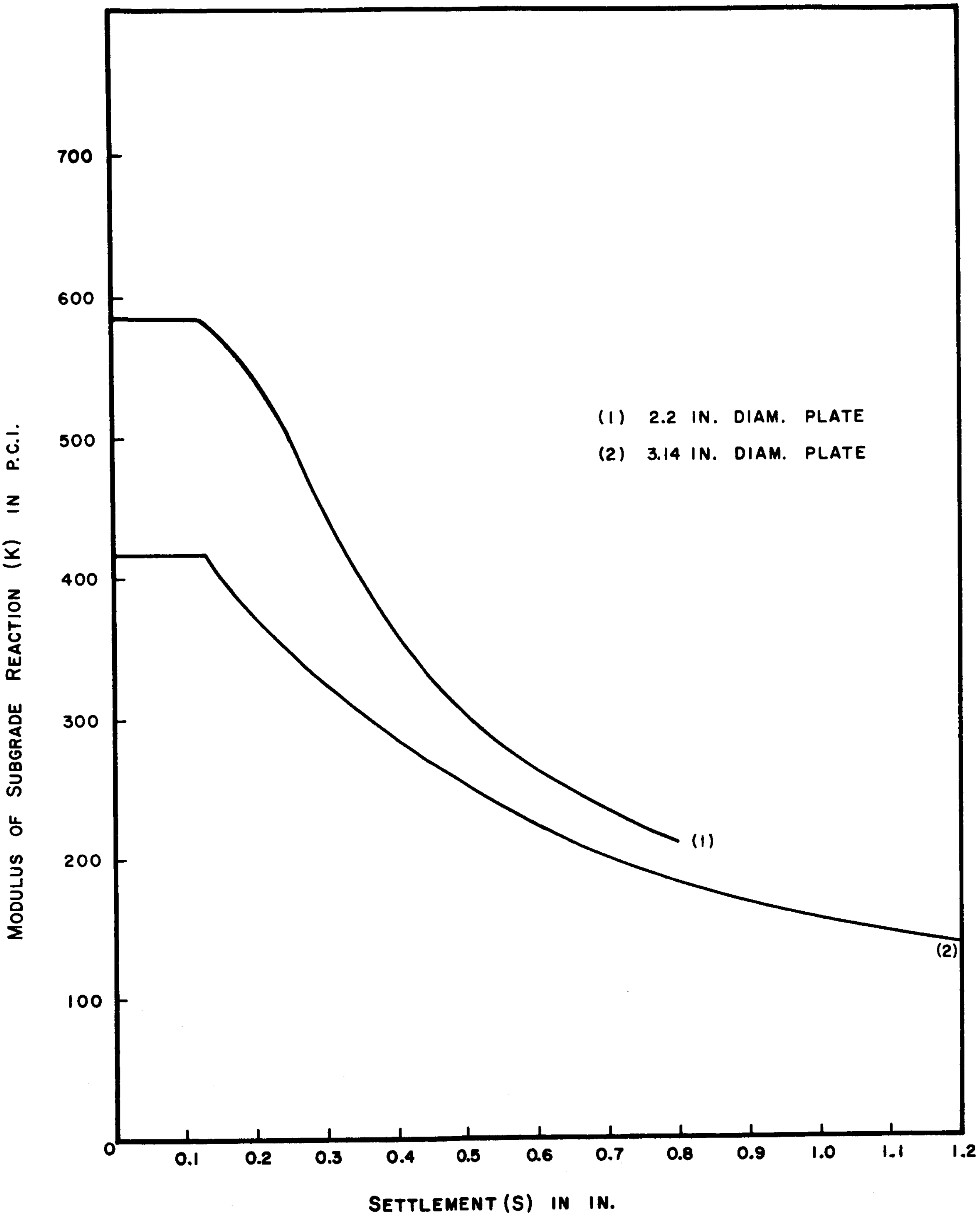

FIG. 8. MODULUS OF SUBGRADE REACTION vs. SETTLEMENT CURVES FOR CIRCULAR PLATES

TABLE 3

THEORETICAL VS. EXPERIMENTAL RESULTS FOR THE CIRCULAR PLATES

B Diameter of Plate, in.	q_o Terzaghi's Theory psi	Ratio of $\frac{q_{o\,Experimental}}{q_{o\,Theoretical}}$	$S_{o \cdot 50}$ Theoretical* Values in.	$S_{o \cdot 50}$ Experimental Values in.	Ratio of $\frac{S_{o \cdot 50\,Experimental}}{S_{o \cdot 50\,Theoretical}}$	B_{Circle} Theoretical** Value lb/cu in.	Ratio of $\frac{k_{Theoretical}}{k_{Experimental}}$
2.22	80.84	1.744	0.0799	0.113	1.414	1340	2.291
3.14	81.18	1.749	0.113	0.182	1.611	948	2.273

* These values are the settlements at 50 percent of the ultimate bearing capacity and are computed using Skempton's equation for immediate settlements.

** These values are determined by correcting Terzaghi's values for a 1.0 x 1.0 footing and a similar clay to values for a circular plate.

where

$S_{0.50}$ = settlement at 50 percent of the ultimate bearing capacity

$\epsilon_{0.50}$ = strain at 50 percent of the maximum stress

B = diameter of plate.

The stress-strain curve used to determine $\epsilon_{0.50}$ was the one determined from the unconfined compression test since the plates were small and were placed at the ground surface.

Values of $S_{0.50}$ determined by Eq 9 are given in Table 3. Values of $S_{0.50}$ determined experimentally and read off the q-S curves are also shown in Table 3. The theoretical values of $S_{0.50}$ determined by Skempton's equation are less than the experimental values. The average ratio between the two values for the plates tested was found to be 1.512. The following are suggested as reasons why the theoretical values of settlement are smaller than the experimental values:

1. The equation derived by Skempton[6] was based on the assumption that Poisson's ratio $\mu = 0.5$. This value is not believed to be representative of the soil conditions in the present investigation, where μ is believed to be much less.

2. Theoretical and experimental results are expected to be in better agreement for footings of larger diameters. The validity of this statement, however, should be checked by more experiments.

Terzaghi[8] recommends values for the modulus of subgrade reaction under a variety of conditions. For the case of stiff pre-compressed clay of unconfined compressive strength equal to 4.0 tons per square foot or more, which is the soil condition in the present investigation, Terzaghi recommends a value of 300 tons per cubic foot for the modulus of subgrade reaction of a

1.0 x 1.0 ft footing on the surface of this clay. This value can be adjusted to any square footing of width B using the following equation:

$$k_B = \frac{k_1}{B} \tag{10}$$

where

k_B = modulus of subgrade reaction for a square surface footing of width B in ft

k_1 = modulus of subgrade reaction, with the same units as k_B, for a 1.0 x 1.0 ft surface footing.

The value of the modulus for a circular surface footing with a diameter B is derived according to the recommendation of Iliya[1] from the equation:

$$k_{B_{circle}} = 0.713\, k_{B_{square}} \tag{11}$$

The theoretical value of k shown in Table 3 is derived by correcting the 300 tons per cubic foot recommended by Terzaghi[8] by applying Eq 10 and Eq 11. The average ratio of the theoretical to experimental values of k for the two circular plates tested was found to be 2.282.

4.2 Results of Tests on Spheres

In this article final results of all tests performed on two spheres, of spherical diameters 3.14 and 5.00 in., are given. An analysis of these results and discussion of their significance is presented. Finally, a comparison with the results of tests on circular plates, and some concluding remarks concerning the prediction of load-settlement behavior for spheres in clay are given.

4.2.1 Load-Settlement Relation

The load-settlement curves for the two spheres are shown in Fig. 9.

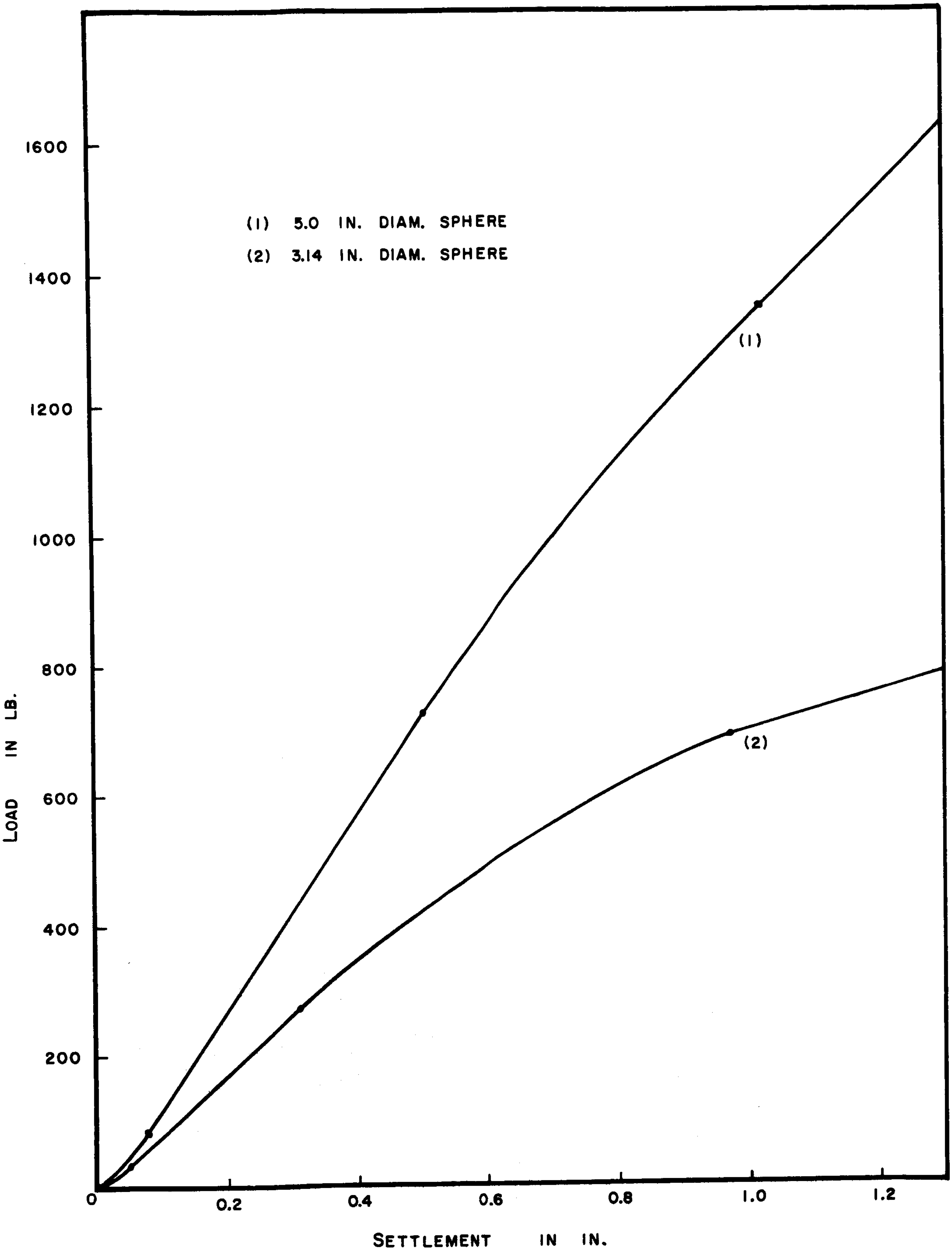

FIG. 9. LOAD VS. SETTLEMENT CURVES FOR SPHERES

The general shape of these curves is the same in both cases, starting with a very small non-linear part where the sphere is not picking up much load, that is, seating itself. The curve then becomes linear for a distance with the load increasing, and then becomes non-linear again. The curve then progresses to a straight line tangent where the load continues to increase at a constant rate. The shape of these curves, with the exception of the initial non-linear seating portion, is very similar to the load-settlement curves for the plates.

Using the same concepts applied for the plates, the shape of these curves indicates a case of local failure condition, where no definite ultimate load could be detected. The ultimate load P_O, however, is chosen at the point of transition of the curve to the final straight line tangent.

Table 4 shows values read off the load-settlement curves for the spheres. S_s is defined as the settlement at the end of the non-linear seating portion of the load-settlement curve, and P_s is the load at this point. S_i is the settlement at the end of the initial straight line portion of the curve, and P_i is the load at this point. S_O is the settlement at which the ultimate load P_O occurs. The slope of the initial straight line portion of the curve is given by the symbol k_i' and that of the final straight line tangent k_f'. These values are given in Table 4a and their ratios, for the two spheres, in Tables 4b and 4c.

The experimental results indicate that the ratio of S_s/B is a constant and has an average value of 0.0161 (see Table 4c). Also the ratio S_i/B is a constant and has an average value equal to 0.0993 for the spheres investigated. Table 4c also shows that the ratio P_s/P_O is not quite constant for both spheres, but that an average of 0.0553 can be taken to represent both cases. The ratio k_i'/B was also constant and equal to about 300 psi.

TABLE 4

LOAD-SETTLEMENT RELATIONS FOR SPHERES

(a) Values Read off Curves

B Diameter of Sphere, in.	S_s in.	P_s lb	S_1 in.	P_1 lb	S_O in.	P_O lb	k_1' lb/in.	k_t' lb/in.
3.14	0.051	33	3.312	275	0.073	693	940	290
5.00	0.080	85	0.496	720	1.022	1350	1500	1000

(b) Ratios

B Diameter of Sphere, in.	Ratio of S_s Referred to the Smaller Sphere	Ratio of P_s Referred to the Smaller Sphere	Ratio of S_1 Referred to the Smaller Sphere	Ratio of P_1 Referred to the Smaller Sphere	Ratio of S_O Referred to the Smaller Sphere	Ratio of P_O Referred to the Smaller Sphere	Ratio of k_1' Referred to the Smaller Sphere	Ratio of k_t' Referred to the Smaller Sphere
3.14	1.000	1.000	1.000	1.000	1.000	1.000	1.000	1.000
5.00	1.569	2.576	1.590	2.618	1.050	1.948	1.596	3.448

TABLE 4 (CONTINUED)

LOAD-SETTLEMENT RELATIONS FOR SPHERES

(c) Ratios

B Diameter of Sphere, in.	Ratio of S_s/B	Ratio of S_1/B	Ratio of S_0/B	Ratio of P_s/P_0	Ratio of P_1/P_0	Ratio of k_1'/k_t'	Ratio of Sphere Diameters Referred to Smaller One	Ratio of k_1'/B psi
3.14	0.0162	0.0994	0.3099	0.0476	0.397	3.24	1.000	299.3
5.00	0.0160	0.0992	0.2044	0.0630	0.480	1.50	1.592	300.0

In summary, S_s, S_i, and k_i are directly proportional to the spherical diameter. The ratio of the ultimate loads P_0 for the two spheres is somewhat greater than the ratio of diameters. Also from Table 4, it is observed that the ratios of P_s and P_i for the two spheres is very close to the square of the ratio of the spherical diameters, hence P_s and P_i may be assumed to be directly proportional to the square of the diameter of the sphere.

The relations outlined in this part can be successfully utilized to predict the load-settlement relation of spherical surfaces of various sizes in similar soil conditions, once a load-settlement curve for any sphere in the same soil is given.

4.2.2 Bearing Capacity - Settlement Relation

For a sphere the cross-sectional area at the ground surface and the surface area beneath the ground surface increase constantly with the increase in settlement. The bearing capacity, at any time during the test, may be obtained by dividing the load at this point by the cross-sectional area corresponding to the particular settlement at this time. This means that the shape of the bearing capacity-settlement curve is different than that of the load-settlement curve.

Figure 10 shows the bearing capacity, based on cross-sectional area, versus settlement curve for the two spheres tested. The shape of the two curves was similar, with the curves starting fairly straight, going into a non-linear portion, then changing to straight line tangent with a very small upward slope.

The shape of the curves in this case was considered to indicate a local shear failure condition. The ultimate bearing capacity q_0 was chosen at the point where the curve changes into a flat straight line tangent

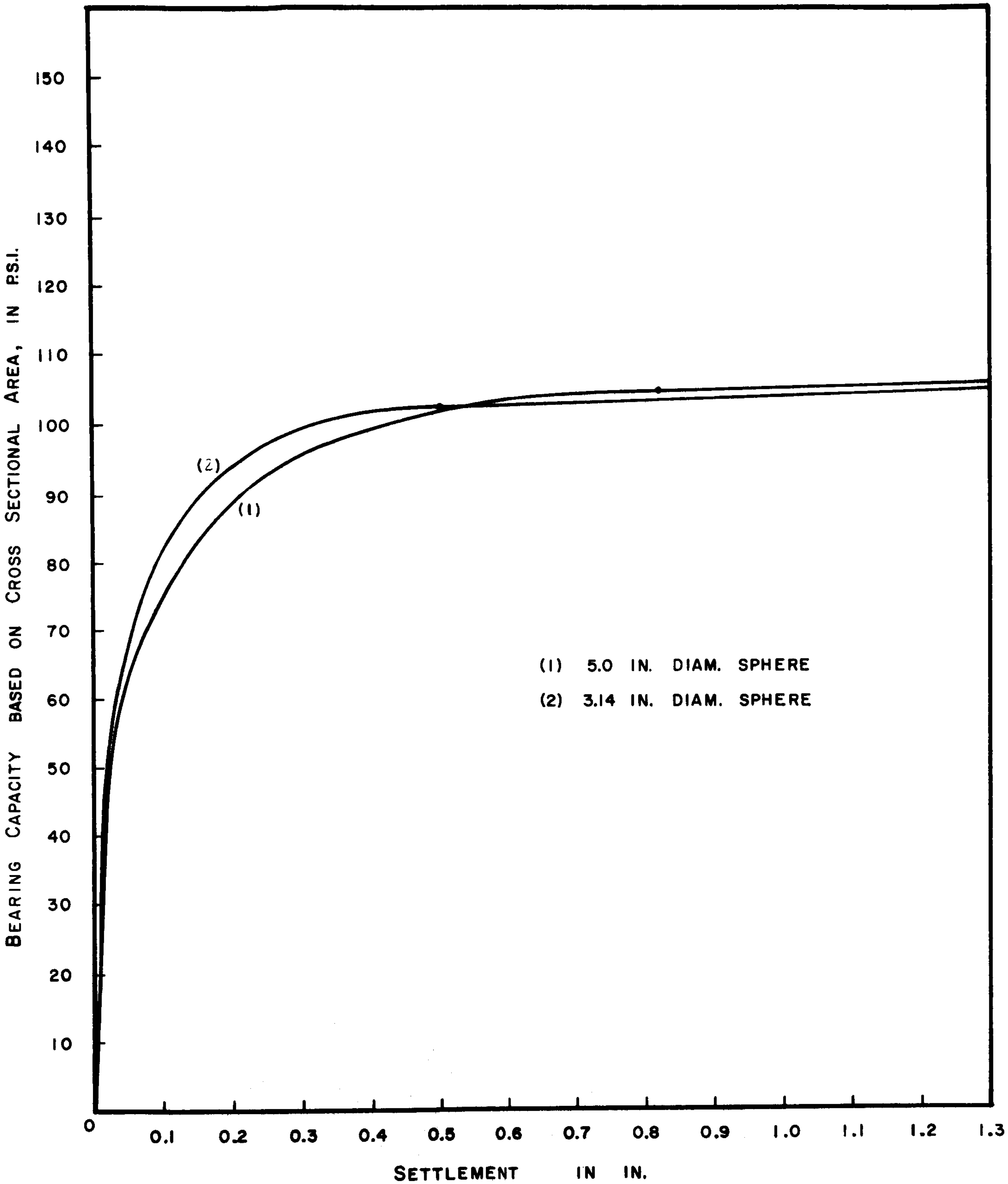

FIG. 10. BEARING CAPACITY (BASED ON CROSS SECTIONAL AREA) VS. SETTLEMENT CURVES FOR SPHERES

It is expected that the curves for general failure conditions will indicate a well defined q_o value and the straight line tangent will be horizontal.

Table 5 shows the value of the ultimate bearing capacity q_o for the two spheres, along with other bearing-capacity, settlement relations. It is seen that q_o for the bigger sphere is slightly higher than that for the smaller sphere. The reason is believed to be the angle of internal friction ϕ of the soil. It is believed that for clays with $\phi = 0$ the ultimate bearing capacity for spheres of various sizes will not depend on the spherical diameters. The ultimate bearing capacity for a sphere in clay is believed to follow the same concepts discussed for plates, with the spherical diameter being substituted for the diameter of the plate in Eq 8.

The settlement S_o, corresponding to the ultimate bearing capacity q_o, is given in Table 5. It can be seen that the ratio of S_o to spherical diameter B is fairly constant and has an average value of 0.162 for the spheres tested. This indicates that S_o is directly proportional to the spherical diameter.

The modulus of subgrade reaction k is defined as the ratio of the bearing capacity, based on cross-sectional area, to the settlement at any point on the q-S curve, that is:

$$k = q/S. \tag{12}$$

Figure 11 shows the variation of k with settlement throughout the test. The similarity in shape between these curves and the ones for the circular plates, Fig. 8, should be noted. The main difference between the two is that for the spheres, the slopes of the initial straight line portion of the bearing capacity-settlement curves were not well defined because of

TABLE 5

BEARING CAPACITY-SETTLEMENT RELATIONS FOR SPHERES

B Spherical Diameter, in.	q_o Ultimate* Bearing Capacity, psi	S_o Settlement at which q_o Occurs, in.	Ratio of q_o Referred to the Smaller Sphere	Ratio of S_o/B	$q_{s\,max}$ Maximum Bearing Capacity psi	S_{max} Settlement in.	Ratio of $q_{s\,max}$ Referred to the Smaller Sphere	Ratio of S_{max}/B	Ratio of S_o/S_{max}	Ratio of $\frac{q_o}{q_{s\,max}}$
3.14	102.6	0.501	1.000	0.1596	89.9	0.314	1.000	0.1000	1.596	1.141
5.00	105.1	0.822	1.024	0.1644	92.2	0.498	1.026	0.0996	1.651	1.140

* q_o is based on the cross-sectional area, that is, $q_o = P_o/A$, where A represents the area of the cross-section at the ground line corresponding to a settlement S_o.

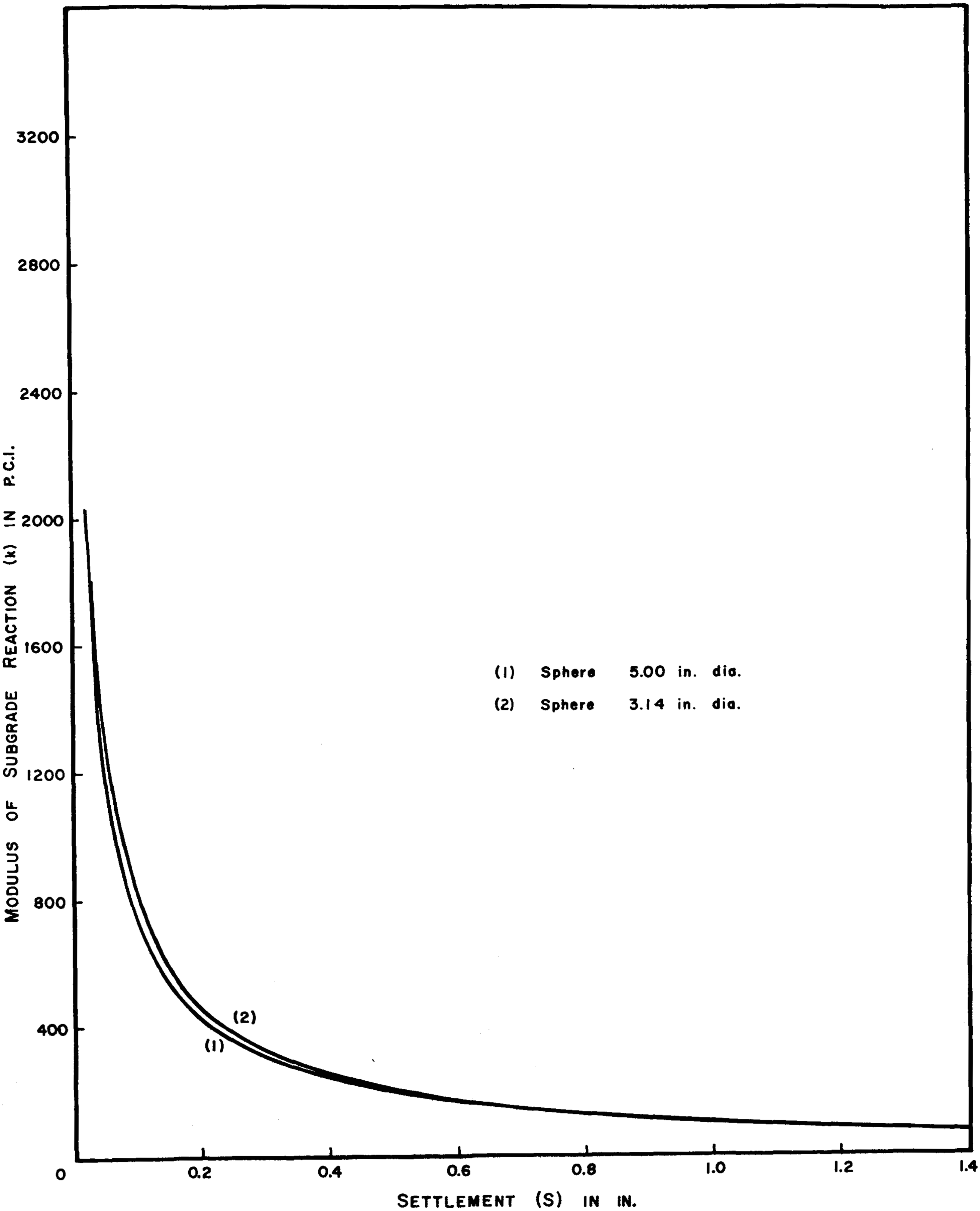

FIG. 11. MODULUS OF SUBGRADE REACTION VS. SETTLEMENT FOR THE SPHERES

the low load readings at the beginning of the test and the insensitivity of the load measuring device. For this reason, the initial constant values of the modulus are not shown in Fig. 11. It must be mentioned here, however, that for spheres, the settlements S_1, at which the constant modulus ends, are less than the ones for circular plates with similar diameters. Figure 11 also points out that the value of the modulus k, at any amount of settlement, is generally higher for the smaller sphere.

Since the cross-sectional area of the sphere at any value of settlement, during the test, is not the actual area in contact with the soil, another definition of bearing capacity for spheres was tried. This definition is that the bearing capacity q_s of the sphere at any time is equal to the load at that moment divided by the surface area of the sphere in contact with the soil at that amount of settlement.

$$q_s = P/A_s \qquad (13)$$

where

q_s = bearing capacity based on surface area of the sphere

P = load

A_s = surface area of the sphere.

Figure 12 shows the curves of q_s versus settlement for the two spheres investigated. The curves start with a fairly straight portion, not very well defined for the reasons mentioned before. The curves peak to a maximum value $q_{s_{max}}$ and then go into a very flat curve, very close to being straight, which slopes downward. The values $q_{s_{max}}$ and the settlement S_{max} at which they occur, for the two spheres, are shown in Table 5.

As indicated in Table 5, the value of $q_{s_{max}}$ is slightly larger for the bigger sphere. The ratio $q_0/q_{s_{max}}$ was constant and equal to 1.14 for

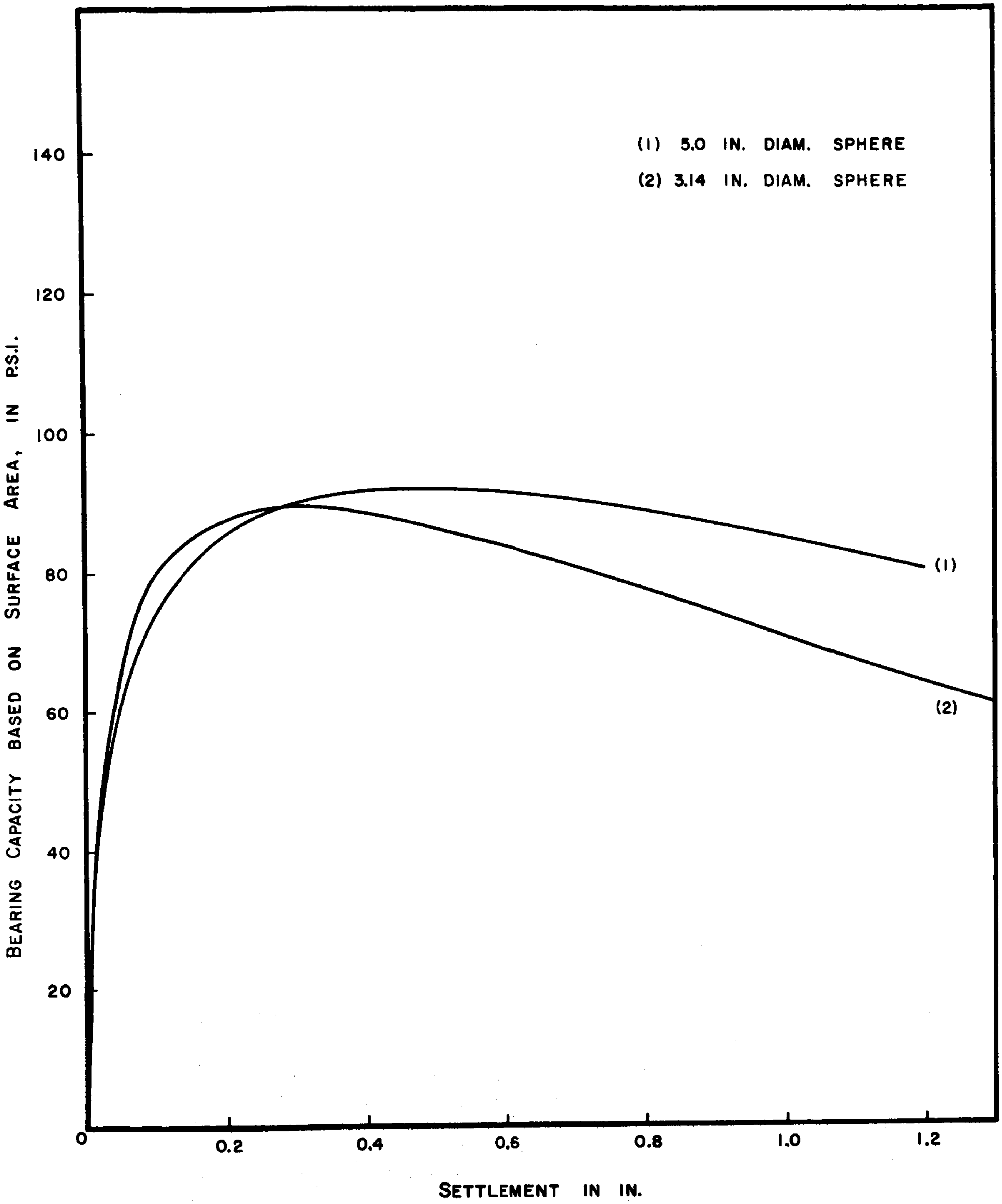

FIG. 12. BEARING CAPACITY (BASED ON SURFACE AREA) VS. SETTLEMENT FOR SPHERES

the two spheres. The settlement S_{max} is larger for the larger sphere. The ratio of S_{max} to the spherical diameter, S_{max}/B, was fairly constant and had an average value of 0.0998 in the present investigation. This indicates that S_{max} is directly proportional to the diameter of the sphere, B. Also, the ratio S_o/S_{max} was apparently constant for the two spheres and equal to an average value of 1.623.

The relations outlined in this part are very helpful in predicting the bearing-capacity, settlement relation for spheres of various sizes in clay soils.

4.2.3 Comparison Between Plates and Spheres

The results of tests performed on the circular plates and spheres are compared together, as shown in Table 6. The ultimate bearing capacity q_o for the 3.14 in. plate was higher than that for the sphere having a spherical diameter equal to the diameter of the plate. The ratio between the value q_o for the 3.14 in. sphere based on the cross-sectional area, to the ultimate bearing capacity of the 3.14 in. plate was equal to 0.723 in the present investigation. This ratio will be used in the next part of this article to develop an empirical equation for predicting the value q_o for spheres in clay.

Table 6 also showed that for the plate and sphere of diameters 3.14 in., the ratio of the settlement S_o at which q_o for the plate occurred to that at which q_o of the sphere occurred was equal to 1.429. Also for these two foundation elements the ratio of the slope of the initial straight line portion of the load-settlement curve for the sphere to that for the plate was 0.291.

The bearing capacity of any sphere at values of settlement where the cross-sectional area of the sphere is equal to the area of a plate

TABLE 6

COMPARISON BETWEEN PLATES AND SPHERES

Foundation Element Tested	q_o Ultimate Bearing Capacity, Based on Cross-Sectional Area psi	Bearing* Capacity of Spheres at an Area Equal to 3.87 sq in. psi	Bearing** Capacity of Spheres at an Area Equal to 7.74 sq in. psi	Ratio of $\frac{q_{o\,sphere}}{q_{o\,plate}}$ (dia. = 3.14 in.)
2.22 in. Plate	141.0	---	---	---
3.14 in. Plate	142.0	---	---	---
3.14 in. Sphere	102.6	102.1	106.0	0.723
5.00 in. Sphere	105.1	93.4	103.1	---

Foundation Element Tested	P_o Ultimate Load lb	S_o Settlement in.	k_1' Slope of the Initial Straight Line Portion of the P. S. Curve lb/in.	Ratio of $\frac{k'_{1\,sphere}}{k'_{1\,plate}}$ (dia. = 3.14 in.)	Ratio of $\frac{S_{o\,plate}}{S_{o\,sphere}}$ (dia. = 3.14 in.)
2.22 in. Plate	547	0.360	2265	---	---
3.14 in. Plate	1099	0.716	3227	---	1.429
3.14 in. Sphere	693	0.501	940	0.291	---
5.00 in. Sphere	1350	0.822	1500	---	---

* This area is equal to the area of the 2.22 in. plate.
** This area is equal to the area of the 3.14 in. plate.

was always less than the ultimate bearing capacity of this particular plate.

The comparisons presented here are but few of the many observations that could be made. The most important items were shown together with examples of some of the lesser important findings.

4.2.4 Prediction of the Ultimate Bearing Capacity of a Sphere in Clay

A semi-empirical approach, based on Terzaghi's theory for bearing capacity and the experimental findings of the present investigation, is followed to develop a method for predicting the ultimate bearing capacity q_o of any sphere, of spherical diameter B, in clay.

The method consists of first determining the ultimate bearing capacity of a circular plate of diameter B, equivalent to the spherical diameter, using Terzaghi's equation No. 8, or the more general equations outlined in Chapter II. The value of the ultimate bearing capacity for the sphere is then derived from the formula:

$$q_{o_{sphere}} = 0.72\, q_{o_{plate}}. \tag{14}$$

This empirical formula was based on the results of this study as summarized in Table 6. Although the ratio 0.72 was derived for a sphere placed at the surface of the soil, it is believed that use of Eq 14 for spheres placed at a small depth will not introduce any objectional error. It must also be pointed out that the ratio 0.72 was derived from results of tests on a silty clay. It is still believed, however, that Eq 14 will work just as well for a clay with $\phi = 0$, as long as q_o for the plate is derived following Terzaghi's recommendations for a clay with $\phi = 0$. Also, it should be emphasized that this procedure will yield values of q_o for spheres that are quite conservative, since the value computed for the plates by Terzaghi's method are on the safe side, as shown before. Values of q_o determined experimentally for spheres will be expected to be somewhere around 1.7 times the values derived by Eq 14.

Eq 14 can be put in a different form as follows:

$$q_{o\,sphere} = 1.3 \left(\frac{2}{3}c\right) N'_{c\,sphere} + 0.3\ \gamma\ B\ N'_{\gamma\ sphere}\ . \tag{15}$$

Equation 15 is for local shear failure conditions and for surface spheres in clay. The bearing capacity factors for the sphere, $N'_{c\,sphere}$ and $N'_{\gamma\ sphere}$, are functions of the angle of internal friction ϕ for the foundation soil. Each of the bearing capacity factors for the sphere is equal to 0.72 times the corresponding bearing capacity factor for the plate determined from Terzaghi's charts[4].

In the preceding discussion some generalization has been made from the results of a very limited number of tests. More experimental data is urgently required to prove this theory and answer all questions in this regard.

The various relations discussed in Art. 4.2 can be used to help predict the load-settlement and bearing capacity settlement behavior of spheres loaded on surfaces of clay. Among the findings, for example, the ratio of the settlement S_o to the spherical diameter B was constant. Also, the slope of the initial straight line portion of the load-settlement curve of a sphere was found to be directly proportional to the spherical diameter and is equal to 0.29. If a load settlement test for a surface sphere of one size is performed on a clay soil, the behavior of spheres of other sizes on the same soil could be predicted using the relation outlined in Art. 4.2. The same concept applies for surface circular plates using the relations discussed in Art. 4.1. The limits for such possibilities have to be determined through tests on elements of various size ranges.

The maximum bearing capacity $q_{s_{max}}$ for a sphere on clay, based on the surface area in contact with the soil, can be predicted from the following empirical relation:

$$q_{s_{max}} = 0.88\ q_0 \tag{16}$$

where q_0 is the ultimate bearing capacity based on cross-sectional area as discussed before.

4.3 Cone Tests

This article includes the results of a limited number of tests on a 60 degree cone. The limited nature of the results obtained indicates that more tests are required, particularly for comparison purposes with cones having angles other than 60 degrees.

4.3.1 Load-Settlement Curve

Figure 13 shows the average load-settlement curve for the tested cone. The curve is non-linear in its entire range with the load always increasing. The initial part of the curve is not very well defined because of the rather small loads that are developed at the beginning of the test and the fact that the 2.0 lb sensitivity of the proving ring is not sensitive enough to read small load values. This will lead to a bearing capacity-settlement curve that is also not well defined at its start.

4.3.2 Bearing Capacity-Settlement Curve

The average curve is shown in Fig. 14. The bearing capacity-settlement curve is non-linear from its start until it finally goes through a fairly straight line tangent with a small upward slope at its end. The

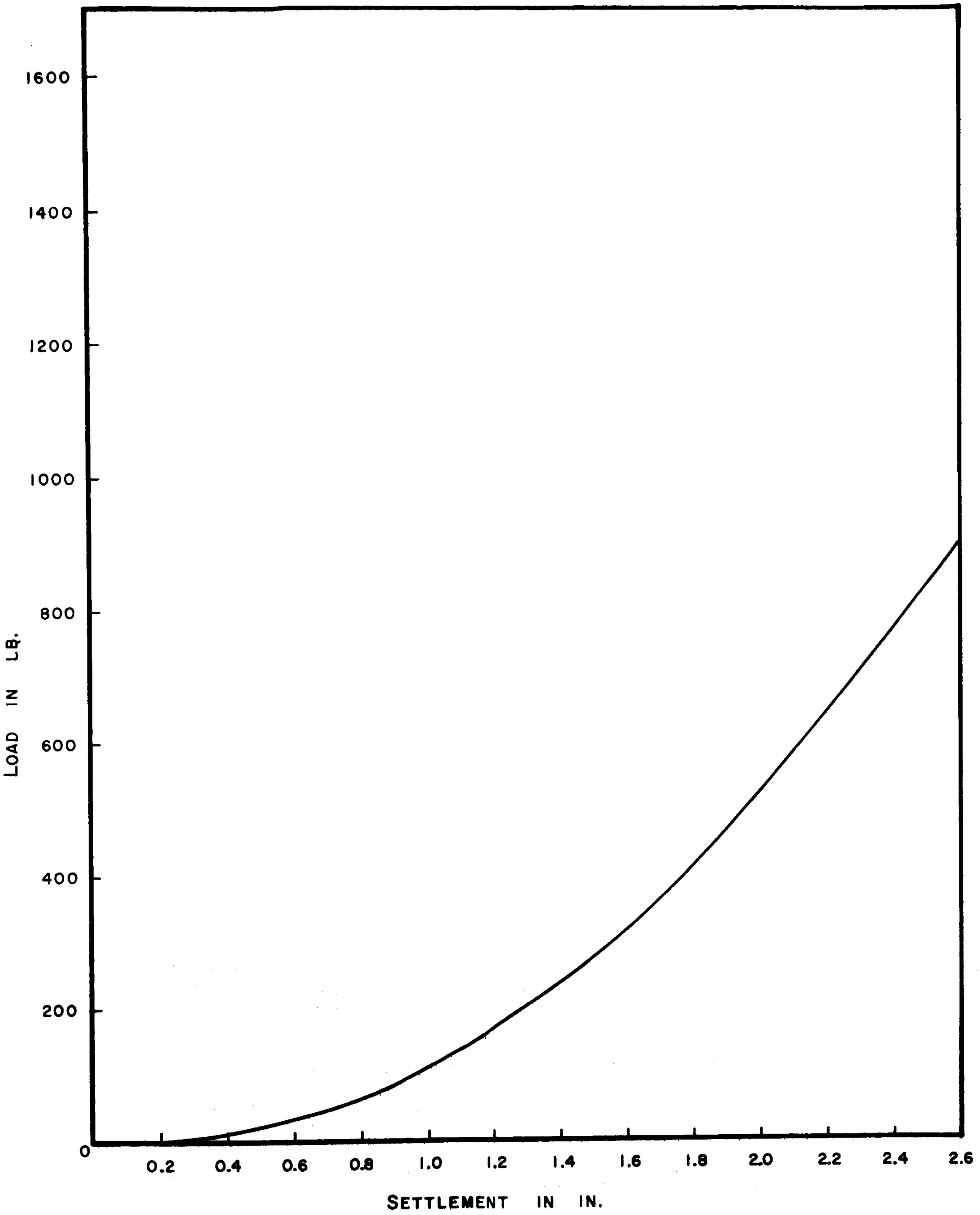

FIG. 13. LOAD — SETTLEMENT CURVE FOR 60° CONE

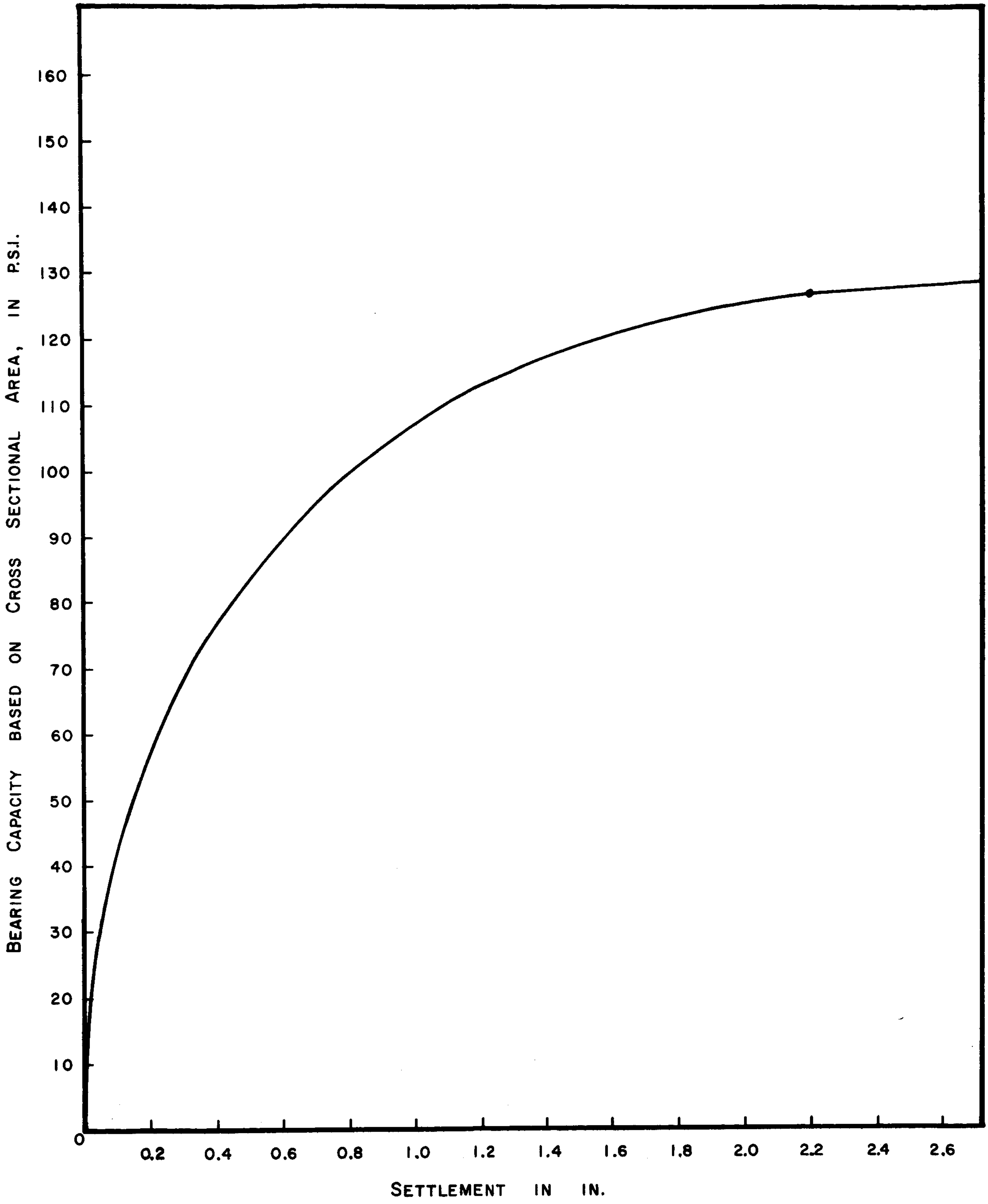

FIG. 14. BEARING CAPACITY VS SETTLEMENT CURVE FOR 60° CONE

point at which the straight line tangent starts is taken to indicate the ultimate bearing capacity of the cone. The slight upward slope of the tangent indicates local shear failure conditions. From Fig. 14 it can be seen that the ultimate bearing capacity of the cone q_o is equal to 127 psi. The settlement S_o at which q_o occurred was found to be 2.2 in.

4.3.3 Comparison of the Results of Tests on the Cone, Plates, and Spheres

The diameter of the cone cross-section at a settlement equal to S_o, 2.2 in., is 2.54 in. The ultimate bearing capacity of a surface circular plate having the same diameter 2.54 in. and in the same foundation soil, determined by Terzaghi's equation, is equal to:

$$q_o = 1.3 \left(\frac{2}{3} \times 2.8\right) 33 + 0.3 \left(\frac{120}{1728}\right) \times 18 \times (2.54)$$

$$= 80 + 0.376 \ (254)$$

$$= 91.0 \text{ psi.}$$

The actual experimental value to be expected from this circular plate, based on the findings of this investigation reported in Table 3, is equal to:

$$q_o \text{ (experimental)} = 91.0 \times 1.746$$

$$= 159 \text{ psi.}$$

This means then that the ratio of the ultimate bearing capacity q_o for a surface cone in clay to the ultimate bearing capacity of a circular surface plate, determined by Terzaghi's equation and modified to indicate experimental value, is equal to 0.799. The diameter of the plate is equal to diameter of the cone cross-section at the ground surface for a settlement equal to that at which the maximum bearing capacity occurred.

For a sphere with a spherical diameter of 2.54 in., the experimental value of q_o to be expected, according to Eq 14 and Table 6, is equal to

$$q_o = 0.72 \times 159 = 114 \text{ psi.}$$

The ratio of q_o of the cone to this value for the sphere is equal to 1.11.

As shown in Table 1, the settlement S_o, at which the ultimate bearing capacity q_o for the circular plates occurred, was proportional to the area of the plate. It then follows for a 2.54 in. diameter plate:

$$S_{o_{plate}} = 0.36 \frac{(2.54)^2}{(2.22)^2} = 0.471 \text{ in.}$$

where 0.36 is S_o for the 2.22 in. plate.

The ratio of S_o for the cone to this value for the circular plate, calculated above, is equal to 4.67.

For circular spheres it can be seen in Table 5 that the ratio S_o/B is nearly constant and equal to 0.162. This means that for a sphere with a spherical diameter equal to 2.54 in., the settlement S_o, at which the ultimate bearing capacity based on cross-sectional area occurred, will be expected to be equal to:

$$S_{o\,(sphere)} = 0.162 \times 2.54 = 0.412 \text{ in.}$$

The ratio of S_o for the cone to that for the sphere, computed above, is equal to 5.34.

Due to the limited amount of data obtained from tests on only one cone, no methods could be arrived at for predicting the ultimate bearing capacity of cones in clay. It is strongly recommended that more tests, on larger cones and cones with other angles, be performed to develop such helpful prediction methods.

CHAPTER V

CONCLUSIONS AND RECOMMENDATIONS

5.1 Conclusions

The results of this experimental investigation showed that:

1. The settlements corresponding to ultimate bearing capacity of circular plates placed at the surface of a clay soil are directly proportional to the surface area of the plates.

2. The ultimate bearing capacity of circular plates on clay follow, in concept, Terzaghi's equation for bearing capacity.

3. The ratio of the ultimate bearing capacity of circular plates on clay determined experimentally to that computed theoretically using Terzaghi's equation was in the average equal to 1.746.

4. The modulus of subgrade reaction, that is, the slope of the initial straight line portion of the bearing capacity-settlement curve for surface circular plates on clay is inversely proportional to the diameter of the plate.

5. The ratio of the value of the theoretical modulus of subgrade reaction for a circular plate on clay as determined using Terzaghi's recommendations, and corrected for the shape and size of the footing, to the value of the modulus determined experimentally was 2.282 in the average.

6. Load-settlement and bearing capacity settlement behavior for spheres on clay can be predicted using the relations outlined in Art. 4.2.

7. The ratio of the settlements defining the ends of the initial straight line portion of the load-settlement curve for a sphere on clay and the slope of this line are all proportional to the spherical diameter.

8. The ratio of the settlement corresponding to the ultimate bearing capacity of a sphere on clay, based on cross-sectional area, or the maximum

bearing capacity of a sphere, based on surface area of contact, is directly proportional to the spherical diameter. The ratio of these two settlements for the spheres tested was a constant and equal to 1.633 on the average. Also, the ratio of the two bearing capacities was about the same for both spheres and averaged 1.14.

9. The ratio of the ultimate bearing capacity of a sphere on the surface of a clay soil, based on its cross-sectional area, to the ultimate bearing capacity of a surface circular plate, on the same soil and having the same diameter as that of the sphere, is equal to 0.72.

10. Limited observations have been made concerning tests on a 60 degree cone, as given in Art. 4.3. No final conclusions have been reached concerning bearing capacities of cones.

REFERENCES

1. Iliya, Raja A. and Reese, Lymon C., "Static Load Versus Settlement for Geometric Shapes on Cohesionless Soil", a report from Department of Civil Engineering, The University of Texas, to National Aeronautics and Space Administration, Langley Research Center, Hampton, Virginia, May 1965.

2. Poor, Arthur R., Cox, William R., and Reese, Lymon C., "Behavior of a Sandy Clay Under Impact of Geometric Shapes", a report from Department of Civil Engineering, The University of Texas, to National Aeronautics and Space Administration, Langley Research Center, Hampton, Virginia, July 1965.

3. Terzaghi, K., Theoretical Soil Mechanics, John Wiley and Sons, Inc., New York, 1943.

4. Terzaghi, K., and Peck, R. B., Soil Mechanics in Engineering Practice, John Wiley and Sons, Inc., New York, 1948.

5. Taylor, D. W., Fundamentals of Soil Mechanics, John Wiley and Sons, Inc., New York, 1948.

6. Skempton, A. W., "The Bearing Capacity of Clays", Proceedings of the Building Research Congress, Div. I, Part III, London, 1951, pp. 180-189.

7. Peck, Hanson, and Thornburn, Foundation Engineering, John Wiley and Sons, Inc., New York, 1957, p. 251.

8. Terzaghi, K., "Evaluation of Coefficients of Subgrade Reaction", Geotechnique, Vol. 5, No. 4, London, Dec. 1955, pp. 297-326.

9. Dawson, R. F., Laboratory Manual in Soil Mechanics, 2nd Ed., Pitman Publishing Co., New York, 1959.

10. Ghazzaly, Osman I., and Dawson, Raymond F., "Laboratory Stress-Deformation Characteristics of Soils Under Static Loading", a report from Department of Civil Engineering, The University of Texas, to National Aeronautics and Space Administration, Langley Research Center, Hampton, Virginia, January 1966.